Agricultural and Forest Meteorology 338 (2023) 109504

Contents lists available at ScienceDirect

Agricultural and Forest Meteorology

journal homepage: www.elsevier.com/locate/agrformet

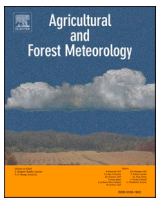

On the variability of the leaf relative uptake rate of carbonyl sulfide compared to carbon dioxide: Insights from a paired field study with two soybean varieties

F.M. Spielmann [a,*], A. Hammerle [a], F. Kitz [a], K. Gerdel [a], G. Alberti [b,c], A. Peressotti [c], G. Delle Vedove [c], G. Wohlfahrt [a]

[a] Institute of Ecology, University of Innsbruck, 6020 Innsbruck, Austria
[b] CNR-IBIMET, via Caproni 8, Firenze, Italy
[c] Department of Agricultural, Food, Environmental and Animal Sciences, University of Udine, 33100 Udine, Italy

ARTICLE INFO

Keywords:
Carbonyl sulfide
Chlorophyll-deficient
Drought stress
Gross primary productivity
Leaf relative uptake
Mesophyll resistance

ABSTRACT

Carbonyl sulfide (COS) has been proposed as a promising tracer for the estimation of the gross primary productivity (GPP) from ecosystem to global scale in recent years. Despite substantial work at spatial scales from leaf to regions, the uncertainty of COS-based GPP estimates are poorly known compared to widely used GPP estimates derived from the net ecosystem CO_2 exchange. One key uncertainty in this context is the leaf relative uptake (LRU) of the COS with respect to the GPP, which must be known a priori. To investigate the influence of environmental factors, like drought, on the variability of the LRU, we conducted an experiment using ecosystem flux measurements of COS, CO_2 and H_2O from two eddy covariance towers above a soybean field, growing a commercial cultivar and a chlorophyll deficient mutant variety, in two separate plots. Our findings suggest that the LRU does not only differ between plant varieties due to differences in the ratio of the internal to ambient CO_2 mole fraction and the internal resistance to COS, but also changes in response to drought. We also found the internal resistance to COS uptake to be a significant factor in controlling the total COS flux for both varieties, but more so for the commercial cultivar. Our study indicates that species-specific differences in the LRU need to be investigated further, and that environmental stress might complicate the usage of COS as a tracer for predicting GPP at ecosystem and global scale.

1. Introduction

At ecosystem level, photosynthesis is referred to as gross primary production (GPP), and it is the main process by which CO_2 enters the biosphere from the atmosphere (IPCC, 2007). However, GPP cannot be measured directly at ecosystem scale. Respiratory processes mask the GPP signal, and only the net ecosystem exchange of CO_2 (NEE) can be measured directly using micrometeorological approaches such as the eddy covariance (EC) method (Aubinet et al., 2000; Baldocchi, 2014). GPP can only be inferred by either applying so called flux partitioning algorithms, which split NEE into GPP and respiration (Lasslop et al., 2010; Reichstein et al., 2005), or more recently developed methods like measuring the sun-induced chlorophyll fluorescence (Parazoo et al., 2014; Rascher et al., 2015; Schlau-Cohen and Berry, 2015), using carbon isotope (Wehr and Saleska, 2015) or carbonyl sulfide (COS) fluxes (Asaf et al., 2013; Campbell et al., 2008; Whelan et al., 2018).

The latter method makes use of the similar pathway of COS and CO_2 into plant leaves as they move through the leaf boundary layer, the stomata and finally the mesophyll to their reaction sites. While CO_2 finds its endpoint at the enzyme Ribulose-1,5-bisphosphate carboxylase-oxygenase (RuBisCO) within the chloroplast stroma (Park and Pon, 1961; Pell, 1979), COS uptake is catalyzed by the enzyme carbonic anhydrase (CA) (ProtoschillKrebs et al., 1996), which is mostly abundant within the cytoplasm as well as the chloroplast stroma (Polishchuk, 2021). In contrast to CO_2, which is rereleased in respiratory processes (van Ingen-Housz, 1779), COS uptake is catalyzed by the CA in a one-way reaction (Protoschill-Krebs and Kesselmeier, 1992), which led to the proposition of COS fluxes as a promising proxy for plant gross uptake of

* Corresponding author.
E-mail addresses: felix.spielmann@uibk.ac.at (F.M. Spielmann), albin.hammerle@uibk.ac.at (A. Hammerle), florian.kitz@uibk.ac.at (F. Kitz), giorgio.alberti@uniud.it (G. Alberti), alessandro.peressotti@uniud.it (A. Peressotti), gemini.dellevedove@uniud.it (G. Delle Vedove), georg.wohlfahrt@uibk.ac.at (G. Wohlfahrt).

https://doi.org/10.1016/j.agrformet.2023.109504
Received 4 January 2023; Received in revised form 3 April 2023; Accepted 9 May 2023
Available online 18 May 2023

CO_2 (Wohlfahrt et al., 2012).

By measuring the COS ecosystem fluxes, and assuming non-plant COS exchange to be negligible or easily modelled, GPP is estimated via Eqn (1):

$$GPP = \frac{F_{COS}}{LRU} \times \frac{\chi_{CO_2}}{\chi_{COS}} \quad (1)$$

Where F_{cos} is the canopy exchange for COS, χ_{COS} and χ_{CO2} are the COS and CO_2 ambient mole fractions, respectively (Sandoval-Soto et al., 2005) and LRU stands for the leaf relative uptake rate of COS with respect to CO_2, i.e. the ratio of the deposition velocities of COS to CO_2.

Mostly lab-based studies have suggested a median value of 1.68 for the LRU of C_3 species, but the 95% confidence interval across all studies lies between 0.7 and 6.2 (Whelan et al., 2018). LRU values based on field studies range from below 0.9 to above 3 (Commane et al., 2015; Kooijmans et al., 2019; Maseyk et al., 2014; Rastogi et al., 2018; Spielmann et al., 2019; Sun et al., 2017). This comparison of LRU values is complicated by the fact that LRU is a function of the incoming photosynthetic active radiation (PAR). While COS is catalyzed by CA in a light-independent process, the uptake of CO_2 by C_3 plants is light-dependent and decreases under low light conditions. Thus, the LRU is higher under lower incoming PAR e.g. in the morning and evening (Kooijmans et al., 2019). It is also important to differentiate between studies at leaf and at canopy scale. LRU at canopy level depends on the species composition as well as the canopy structure, which in turn governs the within-canopy microclimate. Only the top layer of the canopy receives the full incoming PAR. Despite physiological acclimations to the decreasing average light availability within the canopy, LRU should still be larger in deeper layers of the canopy due to the decreased availability in light. Furthermore, relative humidity (RH) and vapor pressure deficit (VPD) will typically increase and decrease, respectively, within the canopy, which in turn would increase the LRU (Kohonen et al., 2020; Sun et al., 2022). In addition, the relative importance of the boundary layer conductance for the leaf COS uptake changes with canopy depth (Wohlfahrt et al., 2012). Therefore, canopy-scale LRUs are expected to be larger than their leaf-scale counterparts.

Further insights into the variability of LRU can be obtained by decomposing Eqn (2) into its underlying driving forces (Wohlfahrt et al., 2012), i.e.

$$LRU = \frac{R_a + aR_b^S + bR_s^S}{R_a + R_b^S + R_s^S + R_i^S} \frac{1}{1 - \chi_i^C/\chi_a^C} \quad (2)$$

Where R_a (m s $^{-1}$) is the aerodynamic resistance, R_b^S (m s $^{-1}$), R_s^S (m s $^{-1}$) and R_i^S (m s $^{-1}$) are the boundary layer, stomatal and internal resistance to COS, with the latter being a combination of the mesophyll and the biochemical resistance for COS. *a* and *b* are the conversion factors for the boundary (0.88) and stomatal (0.83) resistance from COS to CO_2 and χ_i^C/χ_a^C is the ratio of internal to ambient CO_2 mole fractions.

While R_a and R_b are mainly driven by environmental conditions and are typically small during convective daytime conditions (Wehr et al., 2017), R_s^S, R_i^S and χ_i^C/χ_a^C are controlled by plant physiology and might represent major potential sources for variability in LRU (see Eqn (2)). Commonly, χ_i^C/χ_a^C values are between 0.5 and 0.8 (Larcher, 2001; Seibt et al., 2010) for C_3 plants, but may deviate under stress conditions (Ahumada-Orellana et al., 2019). R_i^S was initially thought to be comparatively small, but recent evidence suggests that it may be of similar magnitude as R_s^S (Kooijmans et al., 2019; Sun et al., 2017; Wehr et al., 2017). At present it is unclear if the observed variability in the LRU reflects differences among species or environmental conditions, or both. Additional complications arise from non-leaf, especially soil, contributions to the ecosystem-scale COS exchange, as well evidence for the leaves of certain plant species emitting COS or exhibiting a compensation point (Belvisoet al., 2022; Bloem et al., 2012; Kesselmeier and Merk, 1993; Kitz et al., 2020; Maseyk et al., 2014; Sun et al., 2016). Taken together, despite increasing efforts during the past 15 years (Whelan et al., 2018), it is still unclear whether COS is indeed able to reduce the uncertainty of GPP estimates, in particular compared to the widely applied CO_2 flux partitioning (Lasslop et al., 2010; Reichstein et al., 2005).

The overarching aim of this study was to improve our understanding of the observed variability in LRU. To this end we made use of an experiment (Genesio et al., 2020) in which two soybean varieties, a wild green commercial cultivar (WT) and a naturally occurring chlorophyll-deficient mutant variety (MG), were grown under identical environmental conditions in two adjacent fields. Previous work by Sakowska et al. (2018) has shown that the steady-state photosynthesis of the chlorophyll-deficient variety, despite 80% less chlorophyll, is not different from that of the wild type, while the former transpires significantly less water, apparently due to a higher stomatal resistance. Mesophyll conductance to CO_2 was found to be not significantly different between the two varieties. Integrated over the season, however, biomass and yield of the chlorophyll-deficient variety, are lower, presumably due to less efficient photosynthesis under fluctuating light conditions (i.e. non photochemical quenching relaxation) (Genesio et al., 2020; Sakowska et al., 2018).

Differences between the two soybean phenotypes were investigated using the eddy covariance method (EC) by alternately measuring the CO_2, H_2O and COS ecosystem fluxes of both fields, which minimizes their systematic uncertainty (Ammann et al., 2007). During a rainless period, we were able to investigate the influence of drought and re-wetting following irrigation on the LRUs of the two soybean varieties.

We hypothesized that (H1) differences in LRU between the two cultivars are related to physiological factors such as R_i^S, R_s^S and χ_i^C/χ_a^C rather than R_a and R_b^S, which were expected to be similar due to near-identical environmental conditions between the two adjacent fields and their similar leaf area index (Genesio et al., 2020). We further hypothesized that (H2) the LRU of the two varieties would be similar due to compensating effects (see Eqn (2)) between the higher R_s^S of MG and, since steady-state photosynthesis is similar (Sakowska et al., 2018), supposed lower χ_i^C/χ_a^C ratio of MG, and that (H3) drought would lead to an increase in R_s^S and a decline in the χ_i^C/χ_a^C ratio which in turn, similar to the reasoning implied in H2, would have a cancelling effect on LRU.

2. Material and methods

2.1. Plant material and field site

The measurement campaign took place at a field site in Ariis, Italy (45.87°N, 13.09°E) and lasted from July, 5th to August, 1st, 2017. The commercial green "wildtype" soybean (*Glycine* max L.) (WT) cultivar DekaBig (Dekalb) and the chlorophyll deficient variety MinnGold (MG) were sown on 27th of May in 2017 in two adjacent plots (see Fig. 1& Fig. S1). The reduction of chlorophyll in MG, by approximately 80%, is caused by a naturally occurring nonsynonymous nucleotide substitution of a Mg-chelatase subunit, which is involved in a major step in chlorophyll biosynthesis (Campbell et al., 2014). Even though MG was able to match the rate of photosynthesis of its green wildtype variety in the laboratory (Sakowska et al., 2018), a recent field study (Genesio et al., 2020) reported that the yield of MG was on average 20% lower. The laboratory and the field study found lower photosynthesis of MG under variable light conditions. This has been linked to lower relaxation rates of photoprotection following rapid transitions between illuminated and shaded conditions of MG (Genesio et al., 2020; Sakowska et al., 2018).

Due to a lack of rain during the study period, the field was irrigated twice (July, 17th and 24th).

2.2. General setup

We set up a Quantum Cascade Laser (QCL) Mini Monitor (Aerodyne Research, Billerica, MA, USA) in a container between the two fields (Fig. 1) and measured the ambient mole fractions of CO_2 as well as COS

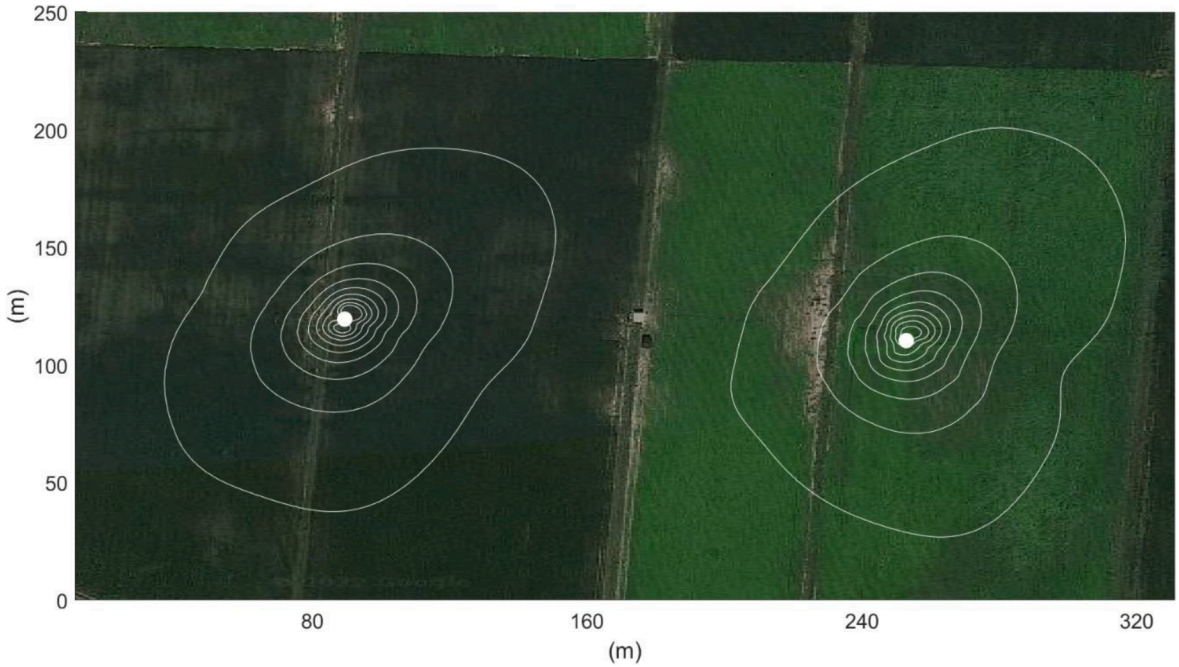

Fig. 1. Satellite image (Google, 2017) of the field site showing the WT plot on the left and the MG plot on the right side. The white dots indicate the position of the eddy towers and the white contour lines depict the 10% to 90% footprint contribution with the container in between them housing the QCL.

by alternately sucking air through two 68 m long 3/8-inch PFA tubes from the EC towers that were placed in the middle of each field (see Fig. 1). H_2O mole fractions were measured using two open path infrared gas analyzers (LICOR 7500A, LI-COR Biosciences, Lincoln, NE, USA) mounted on the eddy mast. The measurement height was 1.75 m. The inlet of each tube was mounted in close proximity to the three-axis sonic anemometers on the eddy mast (CSAT3, Campbell Scientific, Logan, UT, USA), which were used to measure the three velocity components of the wind at each of the fields. Using the eddy covariance method (Aubinet et al., 2000; Baldocchi, 2014) we calculated the ecosystem fluxes for COS, H_2O and CO_2 as described in Gerdel et al. (2017).

2.3. COS soil fluxes

To assess the magnitude of the COS soil exchange, that could mask the canopy COS fluxes, we installed 4 stainless steel rings, with a diameter of 0.032 m^2, 5 cm into the soil one day before the measurements. The rings were placed below the plant canopy and the litter within the soil rings was left untouched. By manually placing a transparent fused silica glass chamber into the water filled channel of a ring, to make an airtight seal, and measuring the COS mole fraction of the ambient air above and within the chambers for 20 to 25 min, we calculated the COS soil flux using the following equation:

$$F = \frac{q(\chi_{cha} - \chi_{amb})}{A} \quad (3)$$

Where F denotes the calculated COS soil flux (pmol $m^{-2} s^{-1}$), q is the flow rate through the chamber in (mol s^{-1}), A is the area of the soil surface within the chamber and χ_{amb} and χ_{cha} are the ambient and chamber mole fractions of COS in ppt, respectively. The measurements were conducted for one day at the start and the end of the campaign. For more details on the setup and calculations see Kitz et al. (2017).

Soil COS fluxes were then modeled on a half-hourly basis using a random forest regression model (Liaw and Wiener, 2002; Virtanen et al., 2020) and subsequently subtracted from the EC—COS fluxes to retrieve the canopy exchange for COS. An analysis of the variable importance identified the photosynthetic active radiation and the soil temperature as the two most important factors controlling the COS soil flux. More information about the model can be found in the supplement (Tables S1 & S2).

2.4. Ancillary data

While we measured soil volumetric water content (0–20 cm) (TDR CS616, Campbell Scientific, Logan, UT, USA) and incoming and outgoing shortwave and longwave radiation (NR01, Four-Component Net Radiation Sensor, Campbell Scientific, Logan, UT, USA) separately at each plot, air- temperature and humidity (HMP45AC, Vaisala, Helsinki, FIN) were measured at a weather station in close proximity to both plots.

The LAI was modelled using the SoySim model (Setiyono et al., 2010, 2007).

2.5. Calculations

2.5.1. Flux partitioning

Separation of NEE into the GPP and the ecosystem respiration (RECO) was done by applying the daytime flux partitioning algorithm of Lasslop et al. (2010). Briefly, the nighttime NEE data, when photosynthesis ceases, was used to determine the temperature response of respiration. The base respiration, as well as the GPP are based on daytime data, where they were modelled using a temperature and a light dependency curve, respectively:

$$NEE = \frac{\alpha\beta R_{PAR}}{\alpha R_{PAR} + \beta} + r_b e^{E_0\left(\frac{1}{T_{ref} - T_0} - \frac{1}{T_{air} - T_0}\right)} \quad (4)$$

Where α (μmol CO_2 μmol^{-1} photons) denotes the canopy light utilization efficiency, β (μmol CO_2 $m^{-2} s^{-1}$) the maximum CO_2 uptake rate of the canopy at light saturation, R_{PAR} (μmol $m^{-2} s^{-1}$) the incoming PAR, r_b is the ecosystem base respiration at the reference temperature T_{ref} (°C), which was set to 15 °C, E_0 (°C) is the temperature sensitivity, T_0 was kept constant at -46.02 °C and T_a is the air temperature.

To account for the vapor pressure deficit (VPD) limiting GPP, the following adjustments are made to β:

$$\beta = \begin{cases} \beta_0 \exp(-k_V(VPD - VPD_0)), & VPD > VPD_0, \\ \beta = \beta_0, & VPD < VPD_0 \end{cases} \quad (5)$$

Where VPD_0 was set to 0,1 kPa (Körner, 1995; Lasslop et al., 2010) and the parameter k_V is estimated.

All parameters of the flux partitioning model, with the exception of E_0, which was calculated by minimizing the root squared mean error, were determined using DREAM, a multichain Markov chain Monte Carlo algorithm (Schoups and Vrugt, 2010; Vrugt and Ter Braak, 2011) as described in Spielmann et al. (2019). While all DREAM outputs were determined for each week, we had to pool all nighttime data to retrieve one value of E_0 for MG and one value for WT across the whole duration of the campaign due to the lack of enough turbulent nighttime data. Only 32% of the eddy covariance nighttime data passed the filters.

2.5.2. Resistances

The internal resistance for COS (R_i^s) was calculated as the difference between the total COS resistance of the canopy (R_t^S) and the sum of all other resistances:

$$R_i^S = R_t^S - \left(R_a^S + R_b^S + R_s^S\right) \quad (6)$$

where R_a (m s $^{-1}$) is the aerodynamic resistance, R_b^S (m s $^{-1}$) the COS boundary layer resistance and R_s^S (m s $^{-1}$) is the stomatal resistance for COS. Since Ri is calculated as the remainder of all other resistances, it will include all measurement and model uncertainties.

R_a (s m $^{-1}$) was calculated using the following equation:

$$R_a = \frac{u}{u^*} + \frac{Phi_m}{ku^*} - \frac{Phi_h}{ku^*} \quad (7)$$

where u is the average horizontal wind speed (m s $^{-1}$), u* the friction velocity (m s $^{-1}$), Phi_m the stability correction factor for momentum, k the dimensionless von Kármán's constant and Phi_h the stability correction factor for heat, which is assumed to be equal to that of water vapor (Hatfield et al., 2005).

We determined boundary layer resistance to water vapor (R_b^W) following Hicks et al. (1987) and Lamaud et al. (2002):

$$R_b^W = \frac{2}{(ku^*)} \frac{Sc^{(2\beta)}}{\Pr}; \quad (8)$$

where Sc and Pr are the dimensionless Schmidt and Prandtl number, respectively.

The stomatal resistance for H_2O (R_s^W) was calculated based on the inverted Penman Monteith (iPM) equation (Monteith and Unsworth, 2013):

$$R_s^W = \left(\frac{\frac{E_w}{VPD_L}}{1 + \frac{E_w}{VPD_L}(R_a + R_b)\left(\frac{Bs}{\gamma - 1}\right)} \right)^{-1} \quad (9)$$

Where E_w is the water vapor flux (kg m $^{-2}$ s $^{-1}$), VPD_L the vapor pressure deficit between the saturated leaf stomatal cavity and the ambient air (kg m $^{-3}$), B the Bowen ratio, s the slope of the saturation vapor pressure curve (kPa K $^{-1}$) and γ the psychrometric constant (kPa K $^{-1}$). Additionally, we also calculated the stomatal resistance using the flux gradient method described in Wehr and Saleska (2021). Since both methods agreed very well (see Fig S3), we used the traditionally applied iPM method. The absolute differences between the two methods can be found in Table S3.

The total COS resistance was calculated using the EC data:

$$R_t^S = \frac{x_{cos}}{F_{cos}} \quad (10)$$

We used the conversion factors from Stimler et al. (2010) to convert the boundary and stomatal resistance for H_2O to COS:

$$R_b^S = R_b^W 1.56 \quad (11)$$

$$R_s^S = R_s^W 1.94 \quad (12)$$

A 95th percentile filter was used on all resistances to remove outliers.

All resistances were converted to the eco-physiological units m^2 s mol^{-1}.

2.5.3. Leaf relative uptake

LRU was calculated via Eqn 1using the GPP resulting from flux partitioning, inferred canopy COS flux and mole fraction data.

Using measured and calculated data, we retrieved the ratio of internal (χ_i^C) to ambient (χ_a^C) CO_2 mole fractions from Eqn (2).

2.5.4. Filtering and statistical analysis

To eliminate the influence of PAR on LRU (Kooijmans et al., 2019), all data in the results section were filtered to be above 800 μmol photons m $^{-2}$ s $^{-1}$. A Kruskal-Wallis and a Bonferroni Post Hoc test were used to compare the medians of the fluxes, the LRU and the resistances between the variants and the phases.

3. Results

3.1. Environmental conditions during study period

The daily air-temperatures ranged from 11.6 to 33.5 °C during our campaign, with higher nighttime temperatures during the first week (Fig. 2a). The one-sided leaf area index (LAI) of both varieties was increasing steadily from about 1 to nearly 4 with WT taking a slight lead over MG for the whole duration (see Fig. 2b). The average soil volumetric water content (SWC) of the top soil layer decreased from 11% at the beginning of the campaign to about 8% after the first week. An ongoing drought decreased the SWC further down to 5% in the second week. The two irrigations in the 3rd and 4th week kept the SWC between 20% and 8%. The daily maximum VPD was above 1.5 kPa for all but 1 day (see Fig. 2c).

Based on the temporal variability of the SWC, we grouped the data into 4 phases: (1) predrought, (2) drought, (3) recovery after the first irrigation and (4) post drought after the second irrigation (see vertical lines in Fig. 2b-c), to investigate the influence of drought on the LRU and the conductances during our 1-month long campaign.

3.2. Fluxes and LRU

Soil contribution to the daytime COS-ecosystem fluxes was minor with a mean of −0.3 pmol m $^{-2}$ s $^{-1}$ and 95% of the soil fluxes between −0.55 and 4.08 pmol m $^{-2}$ s $^{-1}$ (see Fig S2).

During the predrought phase, the median values of the NEE as well as the GPP were statistically not different between WT and MG (see Fig. 3). RECO was statistically significantly lower for WT with a median of 12.0 μmol m $^{-2}$ s $^{-1}$ compared to MG with 14.6 μmol m $^{-2}$ s $^{-1}$ (see Figure S4). The median daytime F_{COS} of MG was higher than WT by 6.3 pmol m $^{-2}$ s $^{-1}$ (13%). The resulting median LRUs of WT and MG were 1.48 and 1.76 (see Fig. 4).

The drought phase affected NEE of WT more strongly than the one of MG with a decline of 42% and 23%, respectively, but we detected no statistically significant difference between the NEE of the two cultivars. The decline in GPP was similar with 30% and 26% for WT and MG, respectively (see Fig. 3). While the RECO of WT was barely affected with a reduction of less than 1%, we observed a decrease of 43% in MG. We measured a decline in median F_{COS} for WT (52%) and MG (30%), which led to a statistically significant difference in F_{COS} between the variants. The drought also induced a reduction in the LRU of WT and MG down to 0.64 and 1.15, which was statistically significant.

In the recovery phase the decline in NEE stopped for WT and NEE

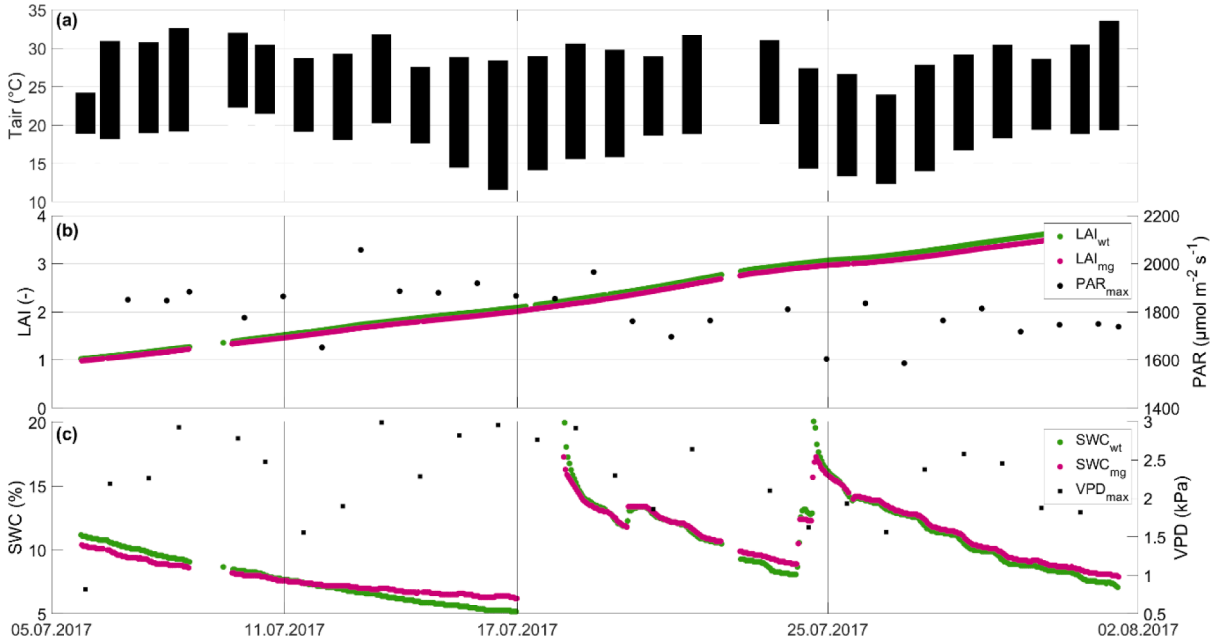

Fig. 2. (a) Bar graphs showing the range of the air temperature at the field (°C), (b) LAI of MG and WT plotted as pink and green, respectively as well as the maximum incoming PAR (µmol photons m^{-2} s^{-1}) on the right Y-axis being depicted by black circles (c) the soil volumetric water content (SWC%) of MG and WT in pink and green respectively plotted on the left Y-axis and the VPD as black squares plotted on the right Y-axis. The 3 black vertical lines separate the 4-phases the data was split into.

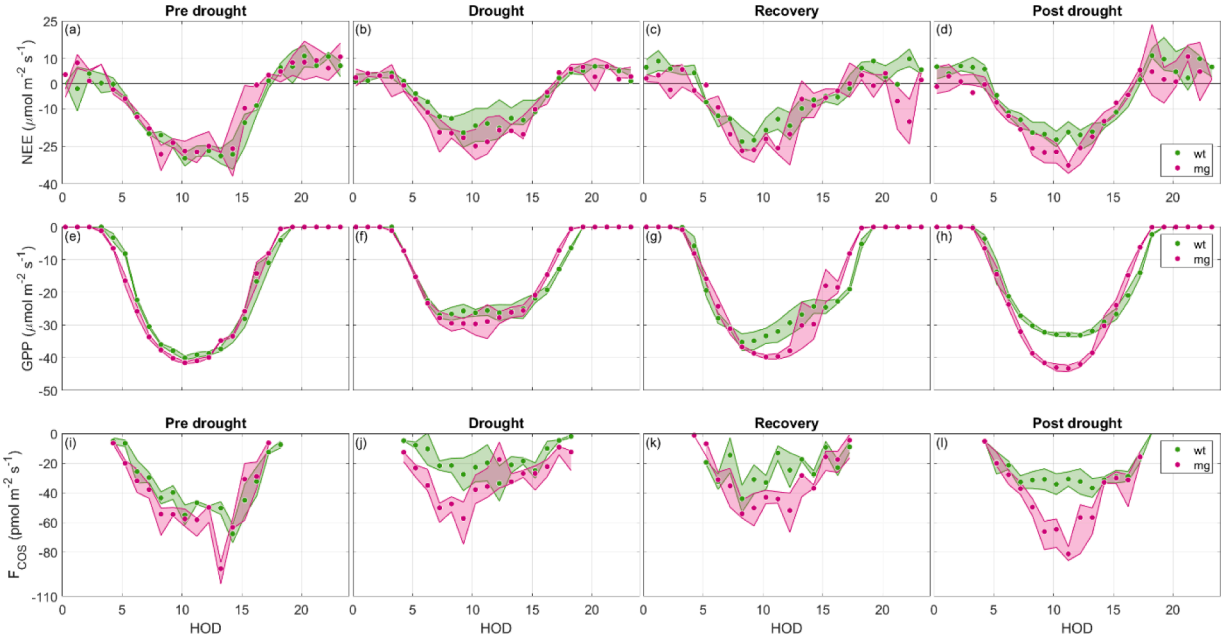

Fig. 3. NEE (µmol m^{-2} s^{-1}) (a-d), GPP (µmol m^{-2} s^{-1}) (e-h) and COS canopy fluxes (pmol m^{-2} s^{-1}) (i-l), where the pink and green circles depict the median diurnal variation for WT and MG respectively. The shaded areas correspond to median absolute deviation of the fluxes. The hour of the day (HOD) is plotted on the X-axis of all subplots.

recovered slightly for MG (see Fig. 3), with GPPs of both variants recovering compared to phase 2 by 20% and 32% for WT and MG, respectively. We observed an increase in RECO for both WT and MG by 4% and 52% up to 17.1 µmol m^{-2} s^{-1} and 12.7 µmol m^{-2} s^{-1}, respectively. F_{COS} further declined by 5% for WT and we observed a recovery by 17% for MG, with the COS fluxes being significantly different during this phase. The LRUs of WT and MG declined further down to 0.43 and 0.78 and were also significantly different from each other (see Fig. 4).

After the second irrigation the NEE as well as the GPP had not recovered for WT. Both fluxes were still 28% and 15% smaller and statistically different from pre-drought values. MG on the contrary had fully recovered in daytime NEE as well as GPP and our analysis indicates no statistically significant difference between the predrought and the post drought phase. While RECO of WT reached pre-drought values (+3%), we observed 15% lower values for MG. F_{COS} was still 30% lower and statistically significantly different for WT compared to the first phase, while it fully recovered for MG, where no statistically significant

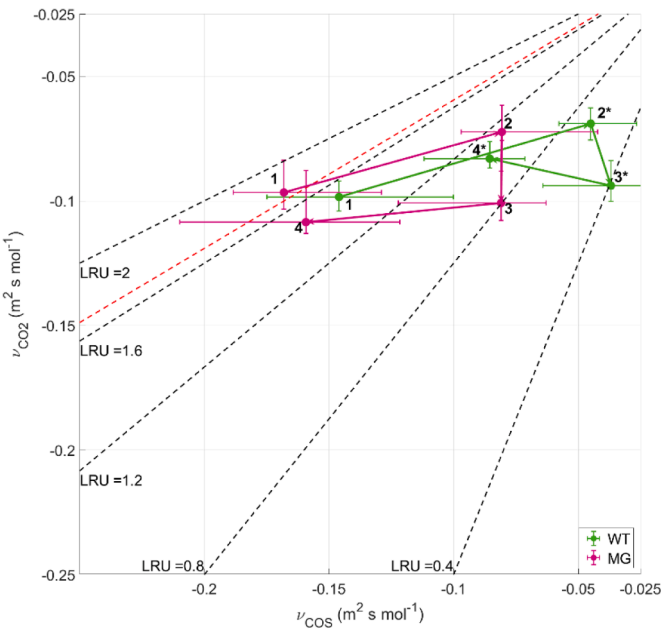

Fig. 4. Median deposition velocities (m^2 s^1 mol^{-1}) for MG and WT under high light conditions (PAR > 800 μmol photons m^{-2} s^{-1}) in pink and green circles respectively. The error bars for the circles depict the 25th and 75th percentile, the numbers indicate the 4 phases, the asterisk beside the numbers indicate a significant difference in the LRU of the respective phase between WT and MG, the pink and green arrows indicate the timeline. The dashed lines indicate the LRUs to the corresponding numbers on the Y and X axis with the median LRU across multiple species of 1.68 stated by Whelan et al. (2018) in red.

difference was detected. LRU also partially recovered in WT as well as MG to 1.03 and 1.59, respectively and statistically different from each other. A detailed table of the statistical differences between variants and the phases of the fluxes and the LRU is reported in Table S4.

3.3. Resistances and internal to external CO_2 mole fraction

The contribution of R_a and R_b to R_{tot} was higher in MG vs WT, with 34% vs. 28%, 17% vs. 8%, 23% vs 8% and 38% vs. 16% from phase 1 to 4, with a higher impact during the pre- and the post-drought phase, where the total resistance was lower compared to the other phases. We observed significant differences in R_a as well as R_b between WT and MG during the recovery and the post-drought phase (see Table S1). Omitting the influence of R_a and R_b would reduce the LRU of WT by 25%, 0%, 25% and 31% and of MG by 45%, 9%, 31% and 37% from phases 1 to 4, respectively.

While median COS resistances under high light conditions during the pre-drought phase were similar for MG and WT, the drought phase caused an increase in the stomatal resistance, especially for WT, which increased from 3.2 to 14.6 m^2 s mol^{-1} (see Fig. 5). The internal resistances for COS also increased in the pre-drought to drought phase transition, from 3.0 to 4.4 m^2 s mol^{-1} and 3.1 to 3.3 m^2 s mol^{-1} for WT and MG respectively.

The ratio of the internal to ambient CO_2 mole fractions χ_i^C/χ_a^C was 0.51 for both varieties and dropped to 0.27 and 0.45 for WT and MG in the drought period, respectively. The correlation of R_s and χ_i^C/χ_a^C can be seen in Figure S5.

After the first irrigation, the stomatal resistances of WT decreased to 5.2 m^2 s mol^{-1}, while it remained higher for MG at 7.0 m^2 s mol^{-1} and we observed a strong increase in the internal resistance for COS of WT to 14.8 m^2 s mol^{-1} overtaking the stomatal resistance as largest resistance. Internal resistance of MG decreased down to 2.7 m^2 s mol^{-1} (see Fig. 5). The χ_i^C/χ_a^C increased to 0.30 and 0.49 for WT and MG, respectively.

After the second irrigation, we observed a decrease in the stomatal to 3.7 and 3.3 m^2 s mol^{-1} and internal resistances to 6.0 and 2.0 m^2 s mol^{-1} for WT and MG respectively. While the internal resistance was still the limiting factor for WT, MG was limited by the stomatal resistance (see Fig. 5). Compared to WT, we observed no statistically significant changes in the internal resistance to COS in MG. χ_i^C/χ_a^C recovered in MG during the post drought phase to 0.52 and increased to 0.63 in WT.

Besides the dissimilar stomatal resistances of WT and MG during the drought, we only observed statistically significant differences for the internal resistance during the recovery and post-drought phase (see

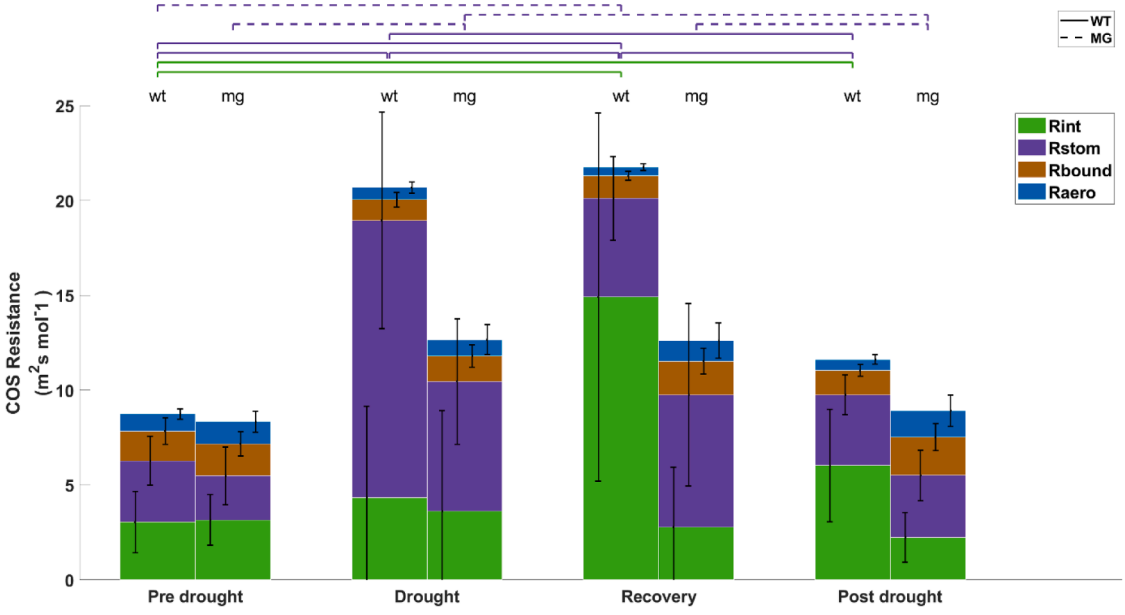

Fig. 5. Median COS resistances under high light conditions (PAR >800 μmol photons m^{-2} s^{-1}) as stacked bar graph for WT and MG and the 4 phases where green bars indicate the internal resistance, purple bars the stomatal resistance, brown bars the boundary layer resistance and blue bars the aerodynamic resistance (m^{2}s mol^{-1}). The black error bars depict the median absolute deviation of the corresponding resistances. The green and purple brackets indicate statistically significant differences between the groups of the internal and the stomatal resistance with the solid and the dashed lines depicting the significance for WT and MG respectively.

Table S1).

4. Discussion

Consistent with H1, R_a and R_b were found to make a small contribution to the difference in the total resistance to COS between the chlorophyll-deficient variety (MG) and the wild type (WT) compared to the physiological resistance components. This result is consistent with the results of Wehr et al. (2017), who also found the impact of R_b to be small compared to the stomatal and internal resistances for COS. Although the non-physiological components were stable for the duration of our measurements and did not impact the difference in LRU between the two cultivars, they still had a large effect on the magnitude of the LRU, especially during the pre- and the post-drought phase, when R_s and R_i were small. The uncertainties of R_a and R_b of the two variants overlap and indicate that the influence of the slight difference in LAI on the canopy aerodynamic properties is small (see Fig. 1). We also expect R_a and R_b to be important for the LRU when comparing the canopy-scale COS uptake of different ecosystems, e.g. forests and grasslands, with different aerodynamic roughness and sites that have predominantly windy or calm conditions.

Also consistent with H1 was that the differences in LRU were largely driven by the differences of R_i, R_s and χ_i^C/χ_a^C. Apart from the drought phase, R_i was surprisingly large and, in all other phases of similar magnitude as R_s. Furthermore, R_i in WT showed high variability and even exceeded R_s during the recovery and the post-drought phase and became the major resistance to COS. The magnitude of R_i was, with the exception of the high R_i of WT during the recovery phase, at the lower end of reported values for sage and hibiscus measured under high light intensity by Stimler et al. (2010).

To date, the high GPP of MG, despite having a lower chlorophyll content, has been attributed to a more even light distribution within the mesophyll and a higher light intensity deeper within the canopy (Sakowska et al., 2018). Higher COS uptake of MG due to a lower R_i indicates a faster internal transport for COS and possibly CO_2, which would also explain the higher χ_i^C/χ_a^C ratio of MG. The lower internal resistance of MG might be related to a higher concentration or activity of CA within the plant leaves, a closer positioning of the chloroplast to the intercellular space or other anatomical traits affecting liquid and gas phase resistance pathways (Momayyezi et al., 2020; Theroux-Rancourt et al., 2021). The increase in R_i of WT during the recovery phase could be a delayed effect of the drought. A study by Perez-Martin et al. (2014) reported that drought caused an increase in R_i for CO_2, with biochemical characteristics and mesophyll conductance being the main limiting factors of photosynthesis and still being of importance during the recovery period. An increased importance of the mesophyll conductance for CO_2 during the recovery phase after a drought has also been found by Galmés et al. (2007). A lower activity of CA could explain the increase in R_i for CO_2 as well as for COS and has been reported by Wang et al. (2016) for rapeseed plants, even though plants also seem to counteract the lower CA activity with an increase in its abundance outside of the chloroplast during the recovery phase, as has been observed for moss, rice, and *Arabidopsis* (Li et al., 2020).

In recent literature for COS, the effect of the leaf internal resistance is still debated (Kohonen et al., 2022; Kooijmans et al., 2019; Wohlfahrt et al., 2012). Our results confirm published findings indicating the importance of the internal resistance to COS, in our case consisting of the internal structure (Wohlfahrt et al., 2012), the enzyme activity and location of the CA (Polishchuk, 2021), in controlling the LRU (Sun et al., 2017; Wohlfahrt et al., 2012). Wohlfahrt et al. (2023) demonstrated that the parameterization of R_i represented the largest source of uncertainty for LRU estimates derived by means of an optimality approach. The internal resistance of COS might also be largely responsible for the spread in LRU that has been highlighted by Whelan et al. (2018).

Our second hypothesis (H2) has to be, at least partially, rejected. LRU did not differ significantly between both varieties during the pre-drought period, this was due to similar R_s and χ_i^C/χ_a^C values, rather than a higher R_s and lower χ_i^C/χ_a^C ratio of MG as expected from the results of Sakowska et al. (2018). However, during all other periods, the LRU of MG was statistically significantly higher compared to WT, which also correlated with a higher χ_i^C/χ_a^C ratio in MG contradicting the leaf level results of Sakowska et al. (2018). Given the RECO of WT was fairly stable between the pre-drought and the recovery phase, the large drop and subsequent increase for MG are suspicious (Fig. 3). Although a decrease in RECO during drought and a subsequent increase after irrigation is expected, the magnitude of the changes, almost 50%, are exceptional (Ingrisch et al., 2020; Ribas-Carbo et al., 2005). Additional flux partitioning model runs with more strictly filtered input data however did not allow pinpointing a systematic problem. We thus interpret the inferred changes in RECO of MG to be indicative of a large uncertainty owing to the low fraction of nighttime data that passed quality control.

Despite expecting the opposite, we also observed a statistically significantly higher R_s in WT compared to MG during the drought phase. The observed LRUs during this study, especially those during and after the drought, were all on the lower end of the values reported in literature (Whelan et al., 2018).

H3 also has to be rejected, as the drought caused a significant decline in the LRUs of both varieties. The drought-induced reduction in χ_i^C/χ_a^C (Tominaga and Kawamitsu, 2015)(see Fig. S5), which in isolation causes the LRU to decrease, apparently outcompeted the concurrent increase in R_s, which in isolation increases the LRU. This should only happen for CO_2 (Evans and von Caemmerer, 1996), since the internal COS mole fraction is assumed to be close to zero (Seibt et al., 2010; Stimler et al., 2010; Wohlfahrt et al., 2012), even during times of negligible R_s, and thus should not change during drought. This assumption has been questioned recently by Belvisoet al. (2022), who found net COS emissions of rapeseed and winter wheat, indicating a non-zero leaf internal COS mole fraction for sulfur-rich plant species and under certain conditions like the ripening stage.

Our results indicate that estimates of GPP using COS-based approaches would currently be overestimated during droughts, if the LRU was not properly adjusted. In respect to the rising probability of occurring droughts (IPCC, 2018), further studies should be conducted to investigate, if other plant species and ecosystems display a more robust LRU during drought and other stress factors, or if COS is an inadequate tracer for GPP under these conditions.

5. Conclusion

The utility of COS as a sensitive proxy for ecosystem-scale GPP relies on a precise understanding of the influence factors on the LRU. We measured the COS and CO_2 ecosystem-scale fluxes of two physiologically different soybean varieties in two adjacent fields under near-identical environmental conditions and observed the influence of drought on their stomatal and internal resistances, the ratio of the internal to ambient CO_2 mole fraction and their subsequent impact on the LRU.

This was to our knowledge the first study to quantify the effect of drought on the LRU and its resistance components on canopy scale. Our observations indicate that drought-induced changes of the χ_i^C/χ_a^C ratio and the resistances R_s and R_i do not necessarily cancel each other out in their effect on LRU, which thus varied with changes in soil water availability. Furthermore, the observed LRU differences between the two soybean varieties, under the same environmental conditions, indicate, that the LRU might be more species-specific than previously thought (Wohlfahrt et al., 2023). Taken together, our results question whether LRU, as initial, mostly leaf-scale data has suggested (Whelan et al., 2018), is conserved enough to allow defensible GPP estimates through the application of Eq. (1). Or whether, as one of the reviewers of this paper put it, in comparison to GPP estimates derived from CO_2 flux partitioning (Lasslop et al., 2010; Reichstein et al., 2005), COS-based GPP estimates just trade in uncertainty in LRU for uncertainty in

RECO (Wohlfahrt and Gu, 2015). Given that CO_2 flux measurements are performed at > 900 sites globally using instruments that are way less costly and much easier to maintain (Baldocchi, 2020; Pastorello et al., 2020), this is a valid question which the small COS community needs to critically address.

CRediT authorship contribution statement

F.M. Spielmann: Validation, Formal analysis, Methodology, Writing – review & editing. **A. Hammerle:** Validation, Formal analysis, Methodology, Writing – review & editing. **F. Kitz:** Validation, Formal analysis, Methodology, Writing – review & editing. **K. Gerdel:** Validation, Writing – review & editing. **G. Alberti:** Validation, Writing – review & editing. **A. Peressotti:** . **G. Delle Vedove:** Validation, Methodology, Writing – review & editing. **G. Wohlfahrt:** Validation, Writing – review & editing.

Declaration of Competing Interest

The authors declare that they have no known competing financial interests or personal relationships that could have appeared to influence the work reported in this paper.

Data availability

https://doi.org/10.5281/zenodo.7915225.

Acknowledgments

We thank the De Eccher Agricultural Farm for having hosted our experiment and Mr Dante Michelan director of the farm. Special thanks to Mr. Diego Chiaba. GA and AP were supported by the Italian Government through the NextGenerationEU funds (DM 737/2021) during the data analysis and manuscript preparation. This study was also financially supported by the Austrian National Science Fund (FWF; contracts P26931, P27176, I03859, and P35737) and the University of Innsbruck (Infrastructure funding by Research Area Mountain Regions to G. W.).

Supplementary materials

Supplementary material associated with this article can be found, in the online version, at doi:10.1016/j.agrformet.2023.109504.

References

Ahumada-Orellana, L., Ortega-Farías, S., Poblete-Echeverría, C., Searles, P.S., 2019. Estimation of stomatal conductance and stem water potential threshold values for water stress in olive trees (cv. Arbequina). Irrigat. Sci. 37 (4), 461–467.
Ammann, C., Flechard, C.R., Leifeld, J., Neftel, A., Fuhrer, J., 2007. The carbon budget of newly established temperate grassland depends on management intensity. Agric. Ecosyst. Environ. 121 (1), 5–20.
Asaf, D., et al., 2013. Ecosystem photosynthesis inferred from measurements of carbonyl sulphide flux. Nat. Geosci. 6 (3), 186–190.
Aubinet, M., et al., 2000. Estimates of the annual net carbon and water exchange of forests: the EUROFLUX methodology. Adv. Ecol. Res. 30 (30), 113–175.
Baldocchi, D., 2014. Measuring fluxes of trace gases and energy between ecosystems and the atmosphere - the state and future of the eddy covariance method. Glob Chang Biol 20 (12), 3600–3609.
Baldocchi, D.D., 2020. How eddy covariance flux measurements have contributed to our understanding of Global Change Biology. Glob Chang Biol 26 (1), 242–260.
Belviso, S., et al., 2022. Carbonyl sulfide (COS) emissions in two agroecosystems in central France. PLoS One 17 (12), e0278584.
Bloem, E., Haneklaus, S., Kesselmeier, J., Schnug, E., 2012. Sulfur fertilization and fungal infections affect the exchange of H2S and COS from agricultural crops. J. Agric. Food Chem. 60 (31), 7588–7596.
Campbell, B.W., et al., 2014. Identical substitutions in magnesium chelatase paralogs result in chlorophyll-deficient soybean mutants. G3 (Bethesda) 5 (1), 123–131.
Campbell, J.E., et al., 2008. Photosynthetic control of atmospheric carbonyl sulfide during the growing season. Science 322 (5904), 1085–1088.
Commane, R., et al., 2015. Seasonal fluxes of carbonyl sulfide in a midlatitude forest. Proc. Natl. Acad. Sci. U.S.A. 112 (46), 14162–14167.
Evans, J.R., von Caemmerer, S., 1996. Carbon dioxide diffusion inside leaves. Plant Physiol. 110 (2), 339–346.
Galmés, J., Medrano, H., Flexas, J., 2007. Photosynthetic limitations in response to water stress and recovery in Mediterranean plants with different growth forms. New Phytologist 175 (1), 81–93.
Genesio, L., et al., 2020. A chlorophyll-deficient, highly reflective soybean mutant: radiative forcing and yield gaps. Environmental Research Letters 15 (7).
Gerdel, K., Spielmann, F.M., Hammerle, A., Wohlfahrt, G., 2017. Eddy covariance carbonyl sulfide flux measurements with a quantum cascade laser absorption spectrometer. Atmos. Meas. Tech. 10 (9), 3525–3537.
Google, 2017. Satellite image of the fieldsite nearby Ariis.
Hatfield, J., Baker, J.M. and Ham, J., 2005. Useful Equations and Tables in Micrometeorology.
Hicks, B.B., Baldocchi, D.D., Meyers, T.P., Hosker, R.P., Matt, D.R., 1987. A preliminary multiple resistance routine for deriving dry deposition velocities from measured quantities. Water Air Soil Pollut. 36 (3), 311–330.
Ingrisch, J., Karlowsky, S., Hasibeder, R., Gleixner, G., Bahn, M., 2020. Drought and recovery effects on belowground respiration dynamics and the partitioning of recent carbon in managed and abandoned grassland. Glob. Chang. Biol. 26 (8), 4366–4378.
IPCC, 2007. Denman, K.L., G. Brasseur, A. Chidthaisong, P. Ciais, P.M. Cox, R.E. Dickinson, D. Hauglustaine, C. Heinze, E. Holland, D. Jacob, U. Lohmann, S Ramachandran, P.L. da Silva Dias, S.C. Wofsy and X. Zhang, 2007: couplings Between Changes in the Climate System and Biogeochemistry. In: Solomon, S., Qin, D., Manning, M., Chen, Z., Marquis, M., Averyt, K.B., et al. (Eds.), Climate Change 2007: The Physical Science Basis. Contribution of Working Group I to the Fourth Assessment Report of the Intergovernmental Panel On Climate Change, (eds.). Cambridge University Press, Cambridge, United Kingdom and New York, NY, USA.
IPCC, 2018. Global warming of 1.5 °C. An IPCC Special Report On the Impacts of Global Warming of 1.5 °C Above Pre-Industrial Levels and Related Global Greenhouse Gas Emission pathways, in the Context of Strengthening the Global Response to the Threat of Climate change, Sustainable development, and Efforts to Eradicate Poverty [V. Masson-Delmotte, P. Zhai, H. O. Pörtner, D. Roberts, J. Skea, P.R. Shukla et al. (eds.)]. In Press.
Kesselmeier, J., Merk, L., 1993. Exchange of carbonyl sulfide (Cos) between agricultural plants and the atmosphere - studies on the deposition of cos to peas, corn and rapeseed. Biogeochemistry 23 (1), 47–59.
Kitz, F., et al., 2017. In situ soil COS exchange of a temperate mountain grassland under simulated drought. Oecologia 1–10.
Kitz, F., et al., 2020. Soil COS exchange: a comparison of three European ecosystems. Glob. Biogeochem. Cycle. 34 (4) e2019GB006202.
Kohonen, K.M., et al., 2022. Intercomparison of methods to estimate GPP based on CO2 and COS flux measurements. Biogeosci. Discu. 2022, 1–30.
Kohonen, K.M., et al., 2020. Towards standardized processing of eddy covariance flux measurements of carbonyl sulfide. Atmos. Meas. Tech. 13 (7), 3957–3975.
Kooijmans, L.M.J., et al., 2019. Influences of light and humidity on carbonyl sulfide-based estimates of photosynthesis. Proc. Natl. Acad. Sci. U. S. A.
Körner, C., 1995. Leaf diffusive conductances in the major vegetation types of the globe (Editors). In: Schulze, E.-D., Caldwell, M.M. (Eds.), Ecophysiology of Photosynthesis. Springer Berlin Heidelberg, Berlin, Heidelberg, pp. 463–490.
Lamaud, E., Carrara, A., Brunet, Y., Lopez, A., Druilhet, A., 2002. Ozone fluxes above and within a pine forest canopy in dry and wet conditions. Atmos. Environ. 36 (1), 77–88.
Larcher, W., 2001. Ökophysiologie der Pflanzen 408. -408 pp.
Lasslop, G., et al., 2010. Separation of net ecosystem exchange into assimilation and respiration using a light response curve approach: critical issues and global evaluation. Glob. Chang. Biol. 16 (1), 187–208.
Li, P., et al., 2020. Translocation of Drought-Responsive Proteins from the Chloroplasts. Cells 9 (1).
Liaw, A., Wiener, M., 2002. Classification and regression by RandomForest. R News 2/3, 18–22.
Maseyk, K., et al., 2014. Sources and sinks of carbonyl sulfide in an agricultural field in the Southern Great plains. Proc. Natl. Acad. Sci. U.S.A. 111 (25), 9064–9069.
Momayyezi, M., McKown, A.D., Bell, S.C.S., Guy, R.D., 2020. Emerging roles for carbonic anhydrase in mesophyll conductance and photosynthesis. Plant J. 101 (4), 831–844.
Monteith, J., Unsworth, M., 2013. Principles of environmental physics: plants, animals, and the Atmosphere: fourth Edition. Principl. Environ. Phys.: Plant. Anim. Atmosph. Fourth Ed. 1–401.
Parazoo, N.C., et al., 2014. Terrestrial gross primary production inferred from satellite fluorescence and vegetation models. Glob. Chang. Biol. 20 (10), 3103–3121.
Park, R.B., Pon, N.G., 1961. Correlation of structure with function in Spinacea oleracea chloroplasts. J. Mol. Biol. 3 (1), 1-IN12.
Pastorello, G., et al., 2020. The FLUXNET2015 dataset and the ONEFlux processing pipeline for eddy covariance data. Sci. Data 7 (1), 225.
Pell, E.J., 1979. Chapter 15 - how air pollutants induce disease. In: Horsfall, J.G., Cowling, E.B. (Eds.), How Pathogens, (Editors). Academic Press, pp. 273–292.
Perez-Martin, A., et al., 2014. Regulation of photosynthesis and stomatal and mesophyll conductance under water stress and recovery in olive trees: correlation with gene expression of carbonic anhydrase and aquaporins. J. Exp. Bot. 65 (12), 3143–3156.
Polishchuk, O.V., 2021. Stress-related changes in the expression and activity of plant carbonic anhydrases. Planta 253 (2).
Protoschill-Krebs, G., Kesselmeier, J., 1992. Enzymatic pathways for the consumption of carbonyl sulfide (COS) by higher-plants. Botanica Acta 105 (3), 206–212.

ProtoschillKrebs, G., Wilhelm, C., Kesselmeier, J., 1996. Consumption of carbonyl sulphide (COS) by higher plant carbonic anhydrase (CA). Atmos. Environ. 30 (18), 3151–3156.
Rascher, U., et al., 2015. Sun-induced fluorescence – a new probe of photosynthesis: first maps from the imaging spectrometer. HyPlant 21 (12), 4673–4684.
Rastogi, B., et al., 2018. Ecosystem fluxes of carbonyl sulfide in an old-growth forest: temporal dynamics and responses to diffuse radiation and heat waves. Biogeosci. Discu. 2018, 1–20.
Reichstein, M., et al., 2005. On the separation of net ecosystem exchange into assimilation and ecosystem respiration: review and improved algorithm. Glob. Chang. Biol. 11 (9), 1424–1439.
Ribas-Carbo, M., et al., 2005. Effects of water stress on respiration in soybean leaves. Plant. Physiol. 139 (1), 466–473.
Sakowska, K., et al., 2018. Leaf and canopy photosynthesis of a chlorophyll deficient soybean mutant. Plant. Cell Environ. 41 (6), 1427–1437.
Sandoval-Soto, L., et al., 2005. Global uptake of carbonyl sulfide (COS) by terrestrial vegetation: estimates corrected by deposition velocities normalized to the uptake of carbon dioxide (CO_2). Biogeosciences 2 (2), 125–132.
Schlau-Cohen, G.S., Berry, J., 2015. Photosynthetic fluorescence, from molecule to planet. Phys. Today 68 (9), 66–67.
Schoups, G., Vrugt, J.A., 2010. A formal likelihood function for parameter and predictive inference of hydrologic models with correlated, heteroscedastic, and non-Gaussian errors. Water Resour. Res. 46, 17.
Seibt, U., Kesselmeier, J., Sandoval-Soto, L., Kuhn, U., Berry, J., 2010. A kinetic analysis of leaf uptake of COS and its relation to transpiration, photosynthesis and carbon isotope fractionation. Biogeosciences 7 (1), 333–341.
Setiyono, T.D., et al., 2010. Simulation of soybean growth and yield in near-optimal growth conditions. Field Crop. Res. 119 (1), 161–174.
Setiyono, T.D., et al., 2007. Understanding and modeling the effect of temperature and daylength on soybean phenology under high-yield conditions. Field Crop. Res. 100 (2), 257–271.
Spielmann, F.M., et al., 2019. Gross primary productivity of four European ecosystems constrained by joint CO(2) and COS flux measurements. Geophys. Res. Lett. 46 (10), 5284–5293.
Stimler, K., Montzka, S.A., Berry, J.A., Rudich, Y., Yakir, D., 2010. Relationships between carbonyl sulfide (COS) and CO2 during leaf gas exchange. New Phytol. 186 (4), 869–878.
Sun, W., Berry, J.A., Yakir, D., Seibt, U., 2022. Leaf relative uptake of carbonyl sulfide to CO(2) seen through the lens of stomatal conductance-photosynthesis coupling. New Phytol. 235 (5), 1729–1742.
Sun, W., Maseyk, K., Lett, C., Seibt, U., 2016. Litter dominates surface fluxes of carbonyl sulfide in a Californian oak woodland. J. Geophys. Res.: Biogeosci. 121 (2), 438–450.
Sun, W., Maseyk, K., Lett, C., Seibt, U., 2017. Stomatal control of leaf fluxes of carbonyl sulfide and CO2 in a Typha freshwater marsh. Biogeosci. Discu. 2017, 1–18.
Theroux-Rancourt, G., et al., 2021. Maximum CO(2) diffusion inside leaves is limited by the scaling of cell size and genome size. Proc. Biol. Sci. 288 (1945), 20203145.
Tominaga, J., Kawamitsu, Y., 2015. Tracing Photosynthetic Response Curves with Internal CO_2Measured Directly. Environ. Contr. Biol. 53 (1), 27–34.
van Ingen-Housz, J., 1779. Experiments upon Vegetables, Experiments upon vegetables discovering their great power of purifying the common air in the sun-shine, and of injuring it in the shade and at night: to which is joined, a new method of examining the accurate degree of salubrity of the atmosphere. Pub P. Elmsly and H. Payne London.
Virtanen, P., et al., 2020. SciPy 1.0: fundamental algorithms for scientific computing in Python. Nat. Method. 17 (3), 261–272.
Vrugt, J.A., Ter Braak, C.J.F., 2011. DREAM((D)): an adaptive Markov Chain Monte Carlo simulation algorithm to solve discrete, noncontinuous, and combinatorial posterior parameter estimation problems. Hydrol. Earth Syst. Sci. 15 (12), 3701–3713.
Wang, L., et al., 2016. Comparative proteomics reveals that phosphorylation of β carbonic anhydrase 1 might be important for adaptation to drought stress in Brassica napus. Sci. Rep. 6 (1), 39024.
Wehr, R., et al., 2017. Dynamics of canopy stomatal conductance, transpiration, and evaporation in a temperate deciduous forest, validated by carbonyl sulfide uptake. Biogeosciences 14 (2), 389–401.
Wehr, R., Saleska, S.R., 2015. An improved isotopic method for partitioning net ecosystem–atmosphere CO2 exchange. Agric. For. Meteorol. 214-215, 515–531.
Wehr, R., Saleska, S.R., 2021. Calculating canopy stomatal conductance from eddy covariance measurements, in light of the energy budget closure problem. Biogeosciences 18 (1), 13–24.
Whelan, M.E., et al., 2018. Reviews and syntheses: carbonyl sulfide as a multi-scale tracer for carbon and water cycles. Biogeosciences 15 (12), 3625–3657.
Wohlfahrt, G., et al., 2012. Carbonyl sulfide (COS) as a tracer for canopy photosynthesis, transpiration and stomatal conductance: potential and limitations. Plant Cell Environ. 35 (4), 657–667.
Wohlfahrt, G., Gu, L.H., 2015. The many meanings of gross photosynthesis and their implication for photosynthesis research from leaf to globe. Plant Cell Environ. 38 (12), 2500–2507.
Wohlfahrt, G., Hammerle, A., Spielmann, F.M., Kitz, F., Yi, C., 2023. Technical note: novel estimates of the leaf relative uptake rate of carbonyl sulfide from optimality theory. Biogeosciences 20 (3), 589–596.